X-621-75-149
PREPRINT

WINTER BULGE AND DIURNAL VARIATIONS IN HYDROGEN INFERRED FROM AE-C COMPOSITION MEASUREMENTS

H. C. BRINTON
H. G. MAYR
W. E. POTTER

JUNE 1975

GODDARD SPACE FLIGHT CENTER
GREENBELT, MARYLAND

WINTER BULGE AND DIURNAL VARIATIONS IN HYDROGEN
INFERRED FROM AE-C COMPOSITION MEASUREMENTS

ABSTRACT

The atomic hydrogen distribution at 250 km during December 1974 solstice has been inferred, considering charge exchange equilibrium, from Atmosphere Explorer-C measurements of $\underline{n}(H^+)$, $\underline{n}(O^+)$ and $\underline{n}(O)$. An empirical model, derived from the observations by least square analysis in terms of spherical harmonics, has the following characteristics: (a) $\underline{n}(H)$ increases by as much as a factor of two between the summer and winter hemispheres, (b) the $\underline{n}(H)$ diurnal variation is largest at the equator where $^{n}max/n_{min}$ = 3.2, the maximum occurring at $03^{h}LT$, and (c) the diurnal variation is larger in the winter hemisphere ($^{n}max/n_{min}$ = 2.6 at +40°) than in the summer ($^{n}max/n_{min}$ = 2.3 at -40°). Similar analysis of the gas temperature derived from $\underline{n}(N_2)$ measurements reveals that all $\underline{n}(H)$ and T_g spherical harmonic coefficients are anticorrelated. Both the diurnal and latitudinal (annual) $\underline{n}(H)$ and T_g amplitudes are in substantial agreement with the "zero flux condition", in which exospheric flow dominates the hydrogen distribution. The observed diurnal phase of $\underline{n}(H)$ with respect to T_g is about one hour, agreeing with theory. During the period of measurement the observed mean global values of T_g and $\underline{n}(H)$ were 800K and 3.6 x 10^5 cm^{-3}, respectively, the latter exceeding the Kockarts-Nicolet model concentration by a factor of two.

WINTER BULGE AND DIURNAL VARIATIONS IN HYDROGEN INFERRED FROM AE-C COMPOSITION MEASUREMENTS

In situ measurements of ion and neutral composition by mass spectrometers on the Atmosphere Explorer-C satellite have been used to infer, for solstice conditions, the latitudinal (annual) and diurnal variations of thermospheric atomic hydrogen. Data for the study were obtained between December 6, 1974 and January 28, 1975, with most observations made during the circular orbit phase of the mission at an altitude of approximately 270 km. Orbit precession during this period permitted the acquisition of data covering a full diurnal cycle.

The concentration of neutral hydrogen has been derived from the chemical equilibrium relationship

$$\underline{n}(H) = \frac{8}{9} \frac{\underline{n}(H^+)}{\underline{n}(O^+)} \underline{n}(O) \qquad (1)$$

[Hanson and Ortenburger, 1961], using essentially simultaneous measurements of $\underline{n}(H^+)$ and $\underline{n}(O^+)$ by the Bennett RF ion mass spectrometer (described by Brinton et al. [1973]) and $\underline{n}(O)$ by the open source neutral mass spectrometer (described by Nier et al. [1973]). The altitude range of measurements from which $\underline{n}(H)$ is derived has been restricted to 230-400 km to insure the validity of equation 1; 97% of the data were actually obtained below 300 km. To aid analysis each $\underline{n}(H)$ value has been normalized to an altitude of 250 km using the gas temperature (T_g) derived from simultaneous mass spectrometer measurements of $\underline{n}(N_2)$ by the method described in Hedin et al. [1974].

The hydrogen database is composed of about 1900 $\underline{n}(H)$ values derived from measurements made on approximately 100 orbits. The

observations cover all local times and longitudes and the geodetic latitude range from -68° to +68°, the AE-C orbital inclination. Measurements made above 70° geomagnetic latitude were excluded from the database to reduce scatter in $\underline{n}(H)$ resulting, we believe, from small-scale structure in temperature, ion composition, or plasma drift. The period of observation was characterized by low solar activity, with an average daily $F_{10.7}$ value of 80; the level of magnetic disturbance was low-to-moderate, with average K_p = 3-.

Observations and Analysis

Figure 1 shows the latitudinal variation of $\underline{n}(H)$ at 250 km altitude for both nighttime and daytime conditions. The nighttime points are all $\underline{n}(H)$ values in the database with local times between 00^h-06^h; this interval was chosen because the observed diurnal $\underline{n}(H)$ maximum occurs at about 03^hLT. The daytime points are those in the range 14^h-20^h LT, centered on the diurnal minimum at 17^h LT. The observed nighttime hydrogen concentrations are higher at all latitudes than the daytime values, and the winter hemisphere concentrations are higher than those of the summer hemisphere during both day and night. Scatter in the data is caused by solar and magnetic activity variations, the wide local time window, and instrument noise.

An empirical model has been used to separate the local time dependent and local time independent components of the observed hydrogen distribution. The model was generated by expanding log $\underline{n}(H)$ in terms of spherical harmonics:

$$\log \underline{n}(H) = a_{00}P^0_0 + a_{10}P_1^0 + a_{20}P_2^0 + (a_{11}\cos\omega t + b_{11}\sin\omega t)P_1^1$$

$$+ (a_{21}\cos\omega t + b_{21}\sin\omega t)P_2^1 + (a_{22}\cos 2\omega t + b_{22}\sin 2\omega t)P_2^2 \quad (2)$$

$$+ a_F (F_{10.7}/100.)P^0_0,$$

where ω is the angular frequency of the earth's rotation, t is local time, and the P_n^m's are spherical harmonic functions. A least square fit to the $\underline{n}(H)$ database, with resulting least square error of ± 0.13, has been used to evaluate the coefficients a_{00} through a_F. The coefficients, with error estimates, are shown in Table 1. Two profiles from the model are shown as solid curves in Figure 1; they describe the latitudinal distribution of hydrogen at the extremes of the $\underline{n}(H)$ diurnal variation, 03^h and 17^h LT.

Figure 2 shows the diurnal variation of hydrogen at the equator. All $\underline{n}(H)$ observations between -10° and +10° latitude are plotted against local time, together with the diurnal variation at the equator from the empirical model.

Model profiles of the $\underline{n}(H)$ diurnal component at the equator and at midlatitudes in the winter (northern) and summer (southern) hemispheres are presented in Figure 3. The concentration of hydrogen is observed to be higher throughout the day at midlatitudes in the winter hemisphere than in the summer hemisphere; the difference is about a factor of 1.6 at 03^h LT, the time of the density maximum in $\underline{n}(H)$, and a factor of 1.4 at 17^h LT, when the density is lowest. The curves in Figure 3 also reveal that the amplitude of the diurnal variation is larger at midlatitudes in winter (x2.6) than in summer (x2.3). The observed diurnal amplitude is largest, however, at the equator (x3.2).

The local time-independent (annual) component of $\underline{n}(H)$ variation given by our solstice model is shown in Figure 4. This profile indicates that the hydrogen concentration in the winter hemisphere is as much as a factor of two higher than that in the summer hemisphere

Discussion

The relationship between observed hydrogen concentration and gas temperature at 250 km has been investigated by generating a similar empirical model based on T_g values derived from mass spectrometer $\underline{n}(N_2)$ measurements made simultaneously with the $\underline{n}(H)$ observations. Comparison of the two models reveals that each component of the $\underline{n}(H)$ model, including those associated with season, local time, and solar activity, is inversely correlated with the same component of the T_g model. It should be noted that, when possible, we have compared the T_g values derived from $\underline{n}(N_2)$ with corresponding in situ measurements of T_g from the AE-C neutral atmosphere temperature instrument (described by Spencer et al. [1973]) and with ion temperature (T_i) values from the retarding potential analyzer (described by Hanson et al. [1973]); agreement between the two T_g's is within 5%, and between T_g (N_2) and T_i, 10%.

The relative amplitudes of the midlatitude $\underline{n}(H)$ diurnal variations presented in Figure 3 are qualitatively consistent with corresponding temperature variations obtained from the T_g empirical model. The observed diurnal variation of $\underline{n}(H)$ in the winter hemisphere is a factor of 2.6, corresponding to a 25% daily T_g variation; the summer n(H) diurnal amplitude is smaller (x2.3), and corresponds to a smaller T_g variation of 14%.

These n(H) diurnal variations are higher than the factor of about 1.8 derived by the same technique from Explorer 32 measurements [Brinton and Mayr, 1971, 1972]. This discrepancy may in part be due to the fact that our earlier measurements were made at a higher altitude (350 km). Our present diurnal amplitudes appear consistent with the theoretical model of Tinsley et al. [1975] for minimum solar activity and a thermospheric wind velocity of the order of 100 m s^{-1}. Our results are also consistent with the factor of 2.0 $\pm$ 0.5 n(H) diurnal variation observed at solar minimum by Ho and Moorcroft [1971]. Comparison of our empirical models for hydrogen concentration and gas temperature reveals that the diurnal extremes of the n(H) variation lag those of T_g by about one hour. Earlier observations of such a phase shift include the airglow measurements of Tinsley [1970] and Meier and Mange [1973] and our Explorer-32 results [Brinton and Mayr, 1971, 1972]. The existence of a T_g-n(H) phase lag is a feature of the theoretical models of hydrogen distribution developed by Patterson [1966] and Vidal-Madjar et al. [1974].

The factor of two increase in n(H) between the summer and winter hemispheres (Figure 4) corresponds to a 25% temperature decrease in the T_g empirical model. This n(H) increase is considerably larger than that predicted by the theoretical model of Vidal-Madjar et al. [1974], who based their analysis on the annual temperature variations from Jacchia [1971]. Jacchia's temperatures were inferred, however, from variations in the mass density under the assumption of diffusive equilibrium; this technique underestimates the amplitude of the annual temperature variation by as much as a factor of three [Mayr and Volland, 1972].

The magnitude of the observed "winter hydrogen bulge" is, on the other hand, considerably smaller than the factor of 10-25 observed for the winter helium bulge by OGO-6 [Hedin et al., 1974] and by AE-C [Mauersberger et al., 1975]; we interpret this difference as evidence that exospheric return flow is much more important for determining the seasonal variation of hydrogen than of helium, where thermospheric neutral winds are the dominant factor [Mayr and Volland, 1972; Reber and Hays, 1973].

Figure 5 shows all 1900 $\underline{n}(H)$ values in the database plotted against the gas temperatures derived from simultaneous $\underline{n}(N_2)$ measurements; an inverse relationship between $\underline{n}(H)$ and T_g is clearly indicated. The slope of the line drawn through the data represents the "zero flux condition" from the exosphere theory of Hodges [1973], in which exospheric flow dominates the hydrogen distribution. The agreement between this slope and our observations is further evidence that exospheric flow is the dominant process governing the global distribution of hydrogen.

The mean global temperature at the time of our observations (from Figure 5) was 800K, with a corresponding hydrogen concentration of 3.6 $(10)^5$ cm^{-3} at 250 km. This concentration is approximately a factor of two higher than that given by the Kockarts and Nicolet [1963] theoretical model, a result in substantial agreement with earlier in situ [Brinton and Mayr, 1971, 1972] and airglow [Meier and Mange, 1973; Vidal-Madjar et al., 1973] observations.

Accuracy of Results

Relative variations of $\underline{n}(H)$ can be determined more accurately than absolute concentrations because they are not affected by systematic errors

associated with instrument calibration. We estimate the error in the relative $\underline{n}(H)$ variations presented here as less than 13%, the least square error of the empirical model curve-fit.

Uncertainty in the absolute hydrogen concentrations is estimated to be (+55/-50)%, resulting from possible errors of $\pm$30% in $\underline{n}(H^+)/\underline{n}(O^+)$, $\pm$20% in $\underline{n}(O)$, and (+5/0)% from using equation 1 when $T_i \neq T_g$ [Banks, 1967].

Acknowledgments

We thank J. S. Selekof for the computer programming and graphics support he provided in all phases of this investigation.

REFERENCES

Banks, P. M., The temperature coupling of ions in the ionosphere, Planet. Space Sci., 15, 77-93, 1967.

Brinton, H. C., and H. G. Mayr, Temporal variations of thermospheric hydrogen derived from in situ measurements, J. Geophys. Res., 76, 6198-6201, 1971.

Brinton H. C., and H. G. Mayr, Thermospheric hydrogen: absolute densities and temporal variations deduced from in situ measurements, Space Res., 12, 751-764, 1972.

Brinton, H. C., L. R. Scott, M. W. Pharo, III, and J. T. Coulson, The Bennett ion-mass spectrometer on Atmosphere Explorer-C and -E, Radio Science, 8, 323-332, 1973.

Hanson, W. B., and I. B. Ortenburger, The coupling between the protonosphere and the normal F-region, J. Geophys. Res., 66, 1425-1435, 1961.

Hanson, W. B., D. R. Zuccaro, C. R. Lippincott, and S. Sanatani, The retarding-potential analyzer on Atmosphere Explorer, Radio Science, 8, 333-339, 1973.

Hedin, A. E., H. G. Mayr, C. A. Reber, N. W. Spencer, and G. R. Carignan, Empirical model of global thermospheric temperature and composition based on data from the OGO 6 quadrupole mass spectrometer, J. Geophys. Res., 79, 215-225, 1974.

Ho, M. C., and D. R. Moorcroft, Hydrogen density and proton flux in the topside ionosphere over Arecibo, Puerto Rico, from incoherent scatter observations, Planet. Space Sci., 19, 1441-1455, 1971.

Hodges, R. R., The differential equation of exospheric lateral transport and its application to terrestrial hydrogen, J. Geophys. Res., 78, 7340-7346, 1973.

Jacchia, L. G., Revised static models of the thermosphere and exosphere with empirical temperature profiles, Spec. Rep. 332, Smithson. Astrophys. Observ., Cambridge, Mass., 1971.

Kockarts, G., and M. Nicolet, L'helium et l'hydrogene atomique au cours d'un minimum d'activite solaire, Ann. Geophys., 19, 370-385, 1963.

Mauersberger, K., D. C. Kayser, W. E. Potter, and A. O. Nier, Seasonal variation of neutral thermospheric constituents in the northern hemisphere, J. Geophys. Res., 80, in press, 1975.

Mayr, H. G., and H. Volland, Theoretical model for the latitude dependence of the thermospheric annual and semiannual variations, J. Geophys. Res., 77, 6774-6790, 1972.

Meier, R. R., and P. Mange, Spatial and temporal variations of the Lyman alpha airglow and related atomic hydrogen distributions, Planet. Space Sci., 21, 309-327, 1973.

Nier, A. O., W. E. Potter, D. R. Hickman, and K. Mauersberger, The open-source neutral-mass spectrometer on Atmosphere Explorer-C,-D, and -E, Radio Science, 8, 271-276, 1973.

Patterson, T.N.L., The diurnal variation of the atomic hydrogen concentration at the base of the exosphere, Planet. Space Sci., 14, 425-431, 1966.

Reber, C. A., and P. B. Hays, Thermospheric wind effects on the distribution of helium and argon in the earth's upper atmosphere, J. Geophys. Res., 78, 2977-2991, 1973.

Spencer, N. W., H. B. Niemann, and G. R. Carignan, The neutral-atmosphere temperature instrument, Radio Science, 8, 287-296, 1973.

Tinsley, B. A., Variations of Balmer-α emission and related hydrogen distributions, Space Res., 10, 582-590, 1970.

Tinsley, B. A., R. R. Hodges, Jr., and D. F. Strobel, Diurnal variations of atomic hydrogen: observations and calculations, J. Geophys. Res., 80, 626-634, 1975.

Vidal-Madjar, A., J. E. Blamont, and B. Phissamay, Solar Lyman alpha changes and related hydrogen density distribution at the earth's exobase (1969-1970), J. Geophys. Res., 78, 1115-1144, 1973.

Vidal-Madjar, A., S. Cazes, and C. Emerich, Influence of the earth's rotation and of possible perturbations, on the exobase and exospheric hydrogen densities, Planet. Space Sci., 1375-1402, 1974.

TABLE 1. $\underline{n}(H)$ Empirical Model

	a_{00}	a_{10}	a_{20}	a_{11}	b_{11}	a_{21}	b_{21}	a_{22}	b_{22}	a_F
Coefficients ($\times 10^2$)	+1280.	+34.5	-25.2	+31.9	+44.2	-1.48	+2.53	+2.64	+1.84	-12.2
Errors ($\times 10^2$)	$\pm$4.0	$\pm$2.0	$\pm$1.3	$\pm$2.2	$\pm$2.0	$\pm$0.72	$\pm$0.66	$\pm$0.78	$\pm$0.68	$\pm$5.0

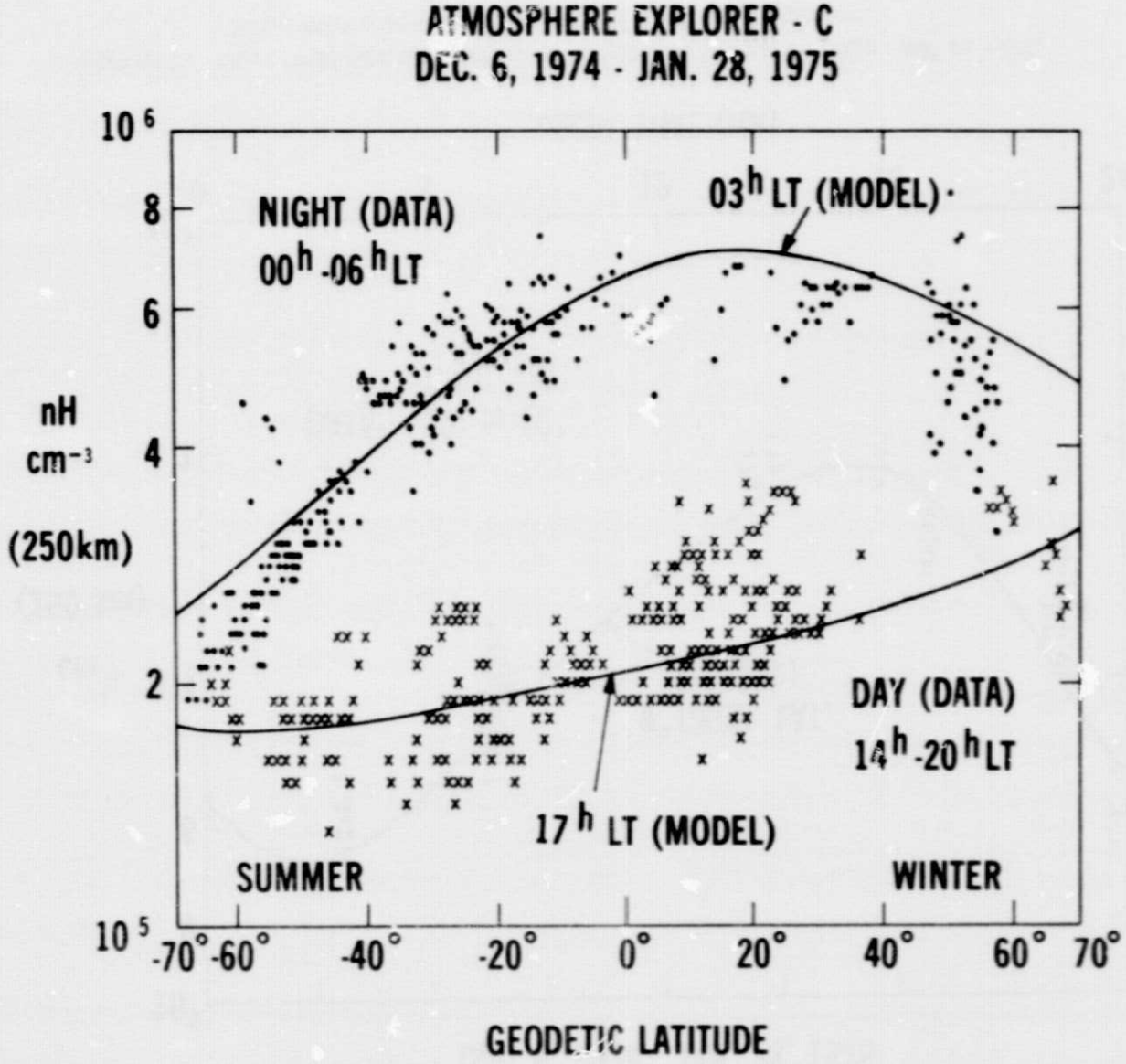

Figure 1. Concentration of atomic hydrogen at 250 km altitude for daytime and nighttime solstice conditions, derived from in situ measurements of ion and neutral composition. Two profiles from the n(H) empirical model are also shown.

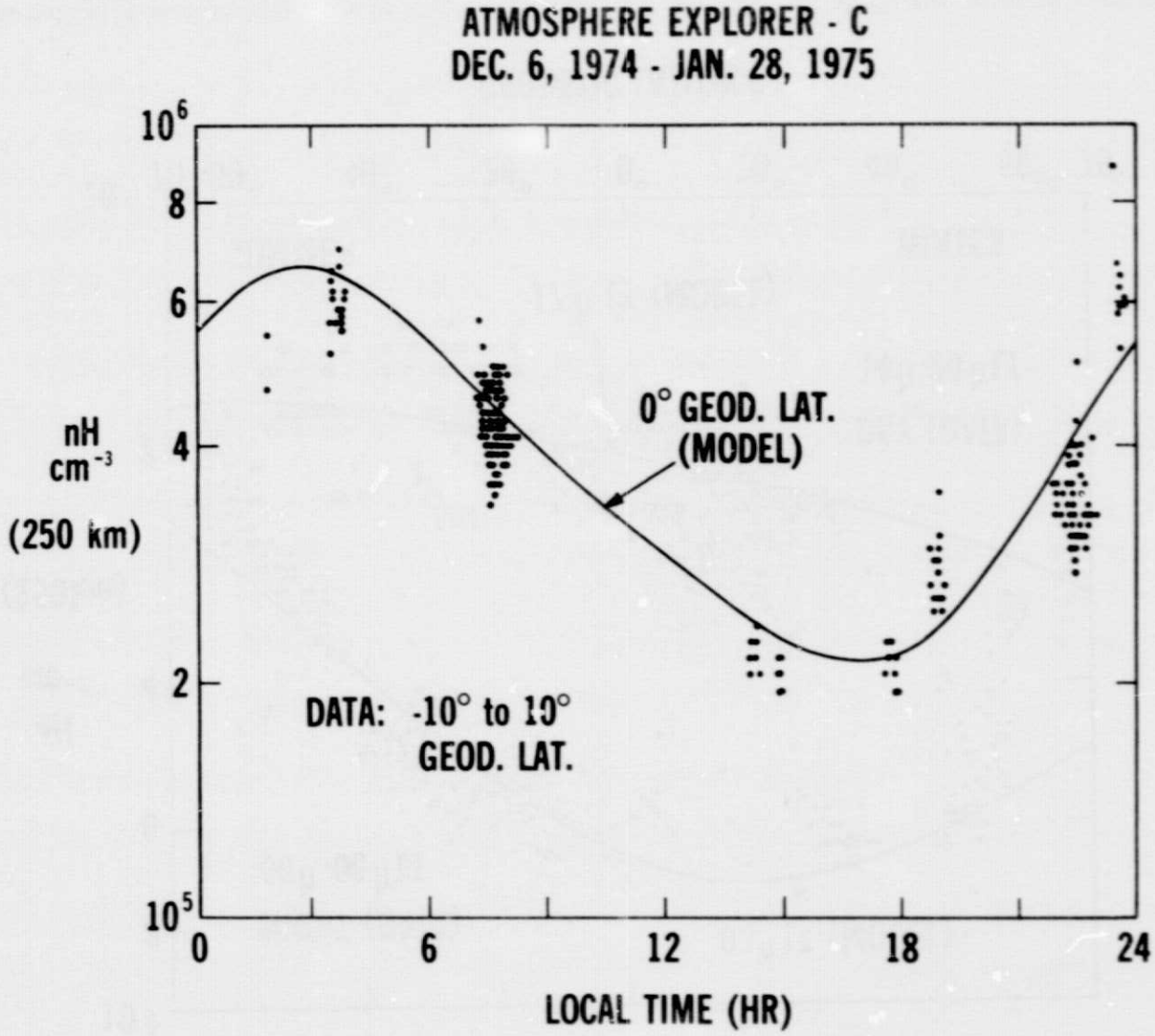

Figure 2. Observed diurnal variation of n(H) in latitude range -10° to +10°. Solid curve is empirical model profile at equator.

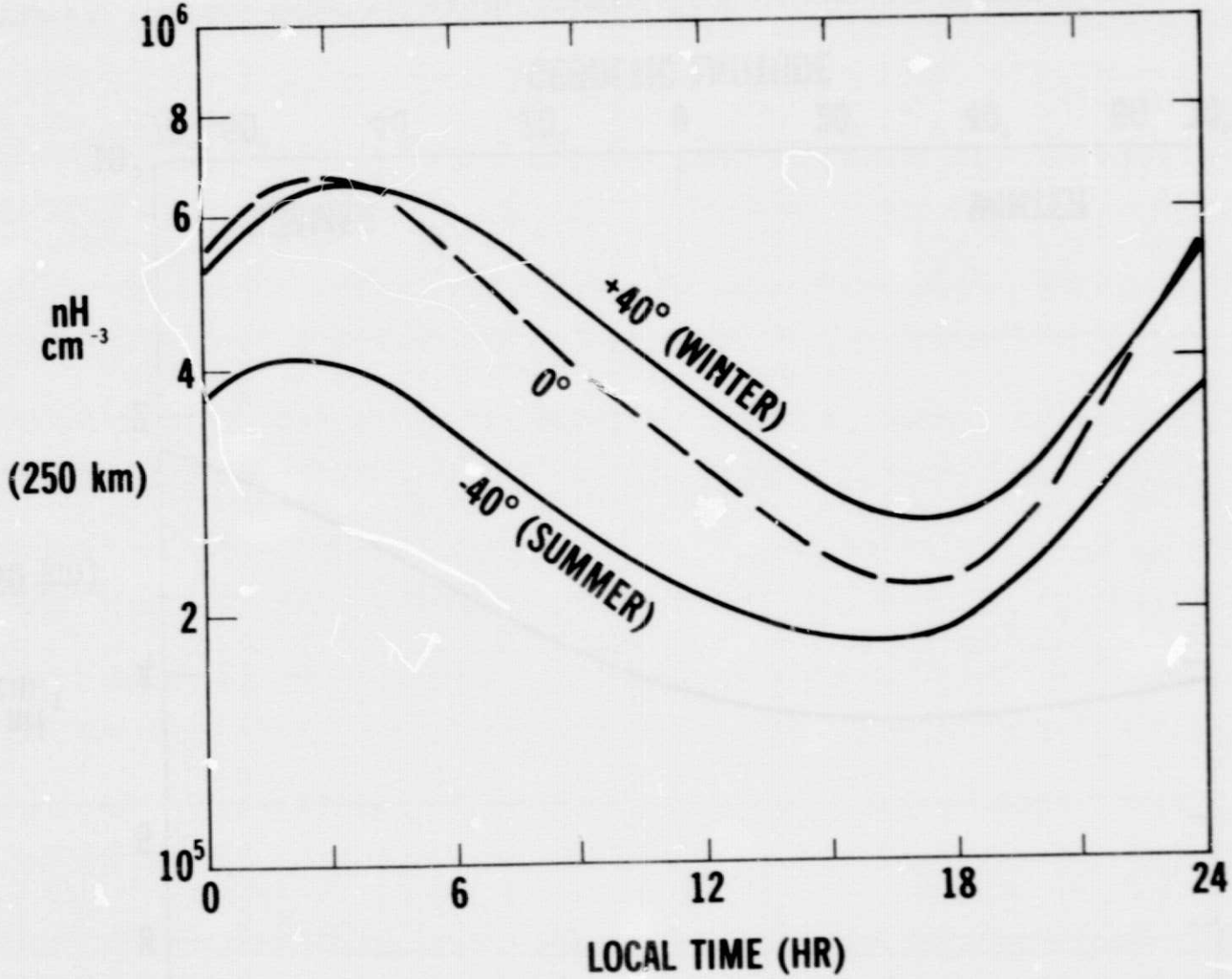

Figure 3. Diurnal variation of n(H) at midlatitudes and at the equator, from the solstice empirical model.

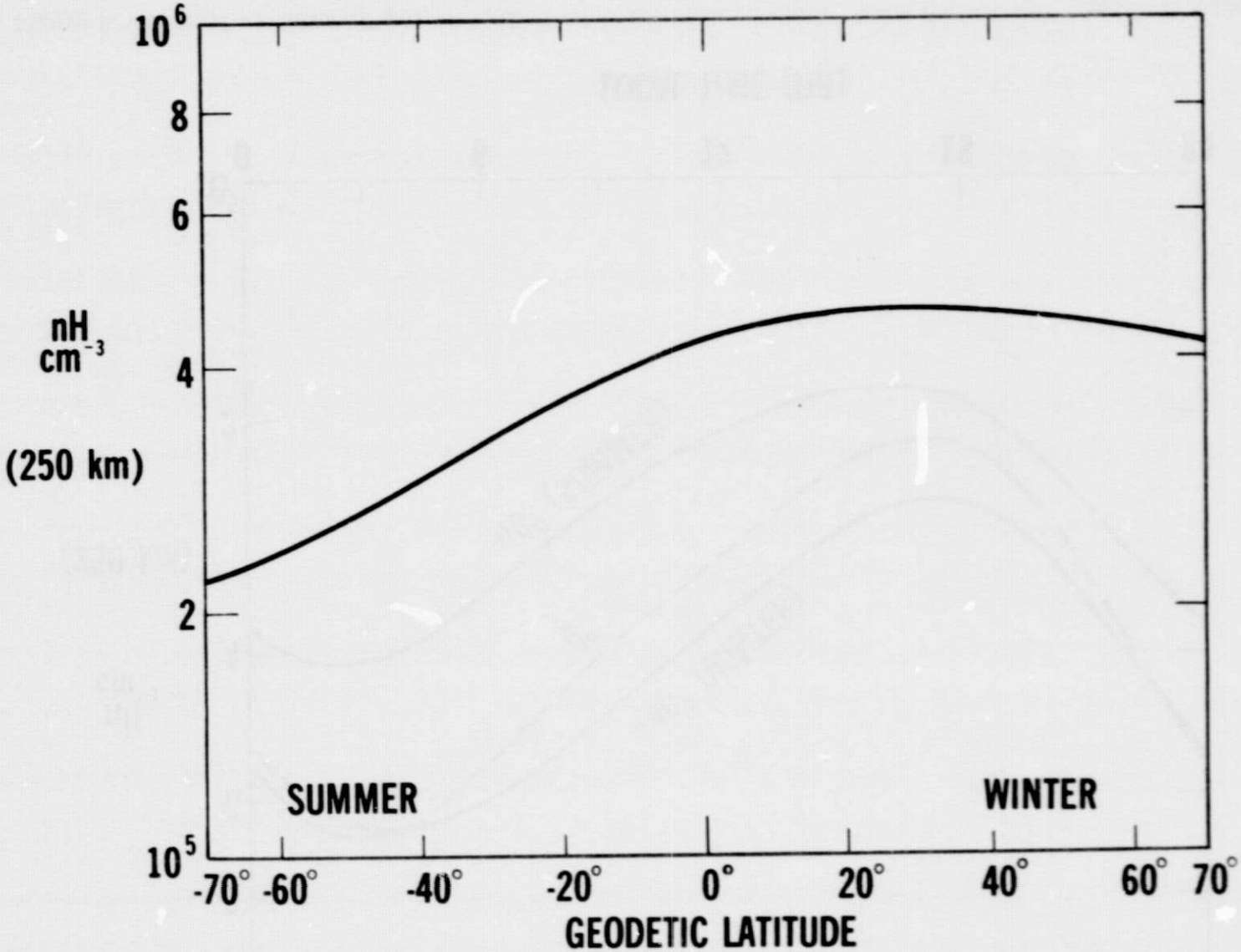

Figure 4. Local time-independent (annual) component of n(H) variation from the solstice model.

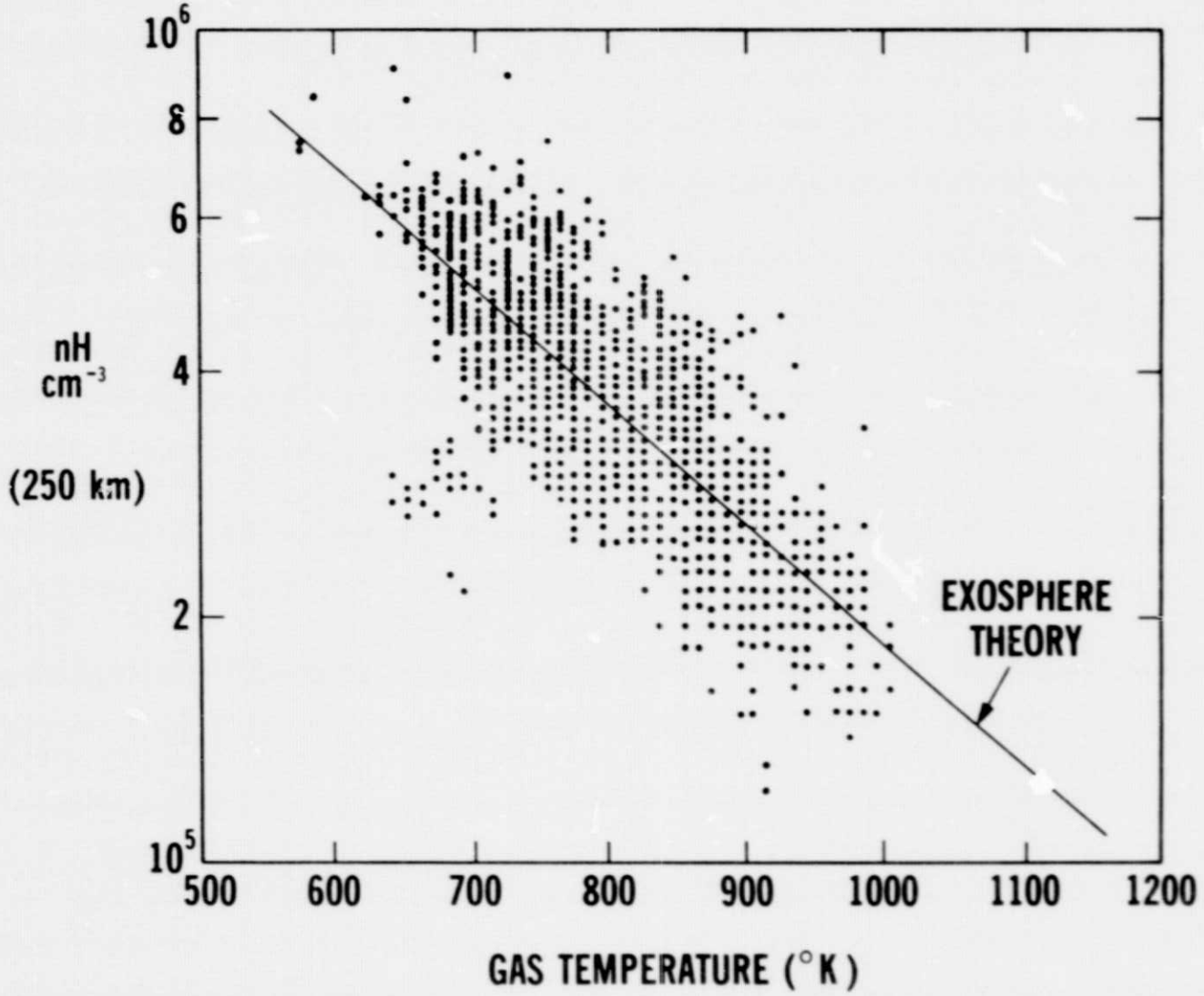

Figure 5. Atomic hydrogen concentrations plotted against gas temperatures derived from simultaneous $\underline{n}(N_2)$ measurements. Slope of line through the data is that given by exosphere theory of Hodges [1973].